On the Propagation of Viscoelastic Waves in a Composite Laminated Plate

J. Feng and Y. M. Haddad*

Dept. of Mechanical Engineering, University of Ottawa
Ottawa, Ontario, Canada K1N 6N5

ABSTRACT

An analytical model is presented to determine the impact response of a viscoelastic laminated composite plate under impact loading. In this context, the "First Shear Deformation Theory" is first used to study the transit wave propagation phenomenon in an analogous linear elastic laminated plate. Subsequently, the "Correspondence Principle" is utilized to extend the obtained elastic solution to a corresponding linear viscoelastic plate of the same geometry. Here, the closed-form displacement solution is obtained in the frequency-domain. The Fast Fourier Transformation (FFT) is, then, applied to invert numerically the arrived-at viscoelastic solution from frequency-domain to time-domain. Microstructural effects such as fibre volume fraction and fibre-aspect-ratio are examined. The obtained results illustrate the importance of including material viscoelasticity in the analysis concerning the prediction of the response of laminated composite plates under impact loading.

1. INTRODUCTION

Laminated composite materials are used extensively in aerospace, automotive and other industries, due to their light weight, high specific modulus, high specific strength and superior design flexibility as compared with traditional materials such as metals. However, the inferior impact properties of these materials represent an obstacle to a wider use in new domains of applications.

Impacts do occur during manufacturing, service operations and maintenance. The situation is even more critical when impacts induce internal damage undetectable by visual inspection. If significant, such damage causes significant increase in local stress and change of natural frequency, which may lead to deterioration in the strength and fatigue life, Therefore, impact analysis of laminated composites has become a subject of active research; e.g., Moon (1975) and Abrate (1991&1994).

---

* Author to whom correspondence should be addressed.

From an impact dynamics point of view, one may assume, for the case of a high velocity impact, that the overall motion of the structure takes place over a time period much larger than the impact contact time. By further assuming that the size of the impactor is much smaller than the least dimension of the specimen or structural member, the analysis of the impact problem would involve the study of the following two distinct topics:

(i) the local mechanics of impact with a deformable half space, and

(ii) the response of the microstructure to a prescribed local impact force as determined in part (i) above.

For the part (ii) of the impact problem, by prescribing the local impact force and the impact duration time, the wave propagation analysis method appears to be convenient in predicting the post impact response of the targeted structure; e.g., Moon (1975).

Within the last four decades, or thereabout, there have been significant efforts directed towards the area of impact wave propagation both analytically, e.g., Moon (1972, 1973 a&b and 1975), Kim and Moon (1977), Sun and Lai (1974), Green and Baylis (1988), Prasad *et al.* (1993), Kam and Chang (1995), and Ma and Huang (1995), and experimentally (e.g., Daniel *et al.*, 1979 and Sun and Wang, 1986). In these works, the elastic composite model was used. Due to the significant influence of the viscoelastic nature of polymeric matrices of composite lamina, it is necessary, however, to treat the polymeric composite laminate as a viscoelastic material whose material properties are, in general, time-, frequency- and temperature-dependent. In this context, there have been so far only few publications directed towards the analysis of the viscoelastic wave propagation phenomenon in laminated composites; e.g., Burtin and Hamelin (1986) and Cederbaum and Aboudi (1989).

Due to the anisotropic and viscoelastic characters of laminated composites of polymeric origin, the pertaining wave propagation problem is much more complex by comparison with its isotropic and/or elastic counterpart. In this, it should be mentioned that both the *approximate plate theory* (e.g., Mindlin and Medick, 1959 and Mindlin, 1961) and first shear-deformation theory (FSDT),Whitney and Pagano (1970), appear to work satisfactorily for the analysis of deformation in anisotropic elastic plates.

The subject of this paper concerns itself with the analytical modelling of wave propagation in a viscoelastic composite plate under impact loading. Here, the complexity of the model increases due to the time-dependency of the problem and, hence, the presence of integro-differential constitutive relations (e.g., Haddad, 1995&2000). In this context, an analytical model is established, in this paper, first in frequency-domain by correspondence to its linear elastic counterpart. Here, the analysis incorporates integral transforms such as Fourier and/or Laplace transforms. The final viscoelastic solution, in time domain, is consequently obtained by inverting the involved integral transform using, for instance, an inversion algorithm of Fast Fourier Transform (IFFT); e.g. Haddad and Feng (2000) and Haddad (2000).

The internal friction (e.g., Kolsky, 1963 and Haddad, 1995) or viscoelastic damping is believed to be responsible for the wave attenuation phenomenon in polymer base composites. It is further recognized that discontinuous fibre reinforced composites have higher damping capacity as compared with the continuous ones, e.g., Gibson and Yau (1980), Gibson *et al.* (1982), Sun *et al.* (1985), Suarez *et al.* (1986), and Feng

(1999). Therefore, the dynamic behaviour under impact loading is investigated in this paper for two material models pertaining to both continuous and discontinuous fibre reinforced composite laminates. In this context, the effects of fibre volume fraction and fibre-aspect-ratio on the dynamic behaviour of composite laminates are also examined.

2. THE MODEL

2.1. Equations of Motion

Consider the symmetric composite laminated plate shown in Figure 1. The latter is of thickness h and is composed of thin material layers which are bonded together as shown in the figure. The material of

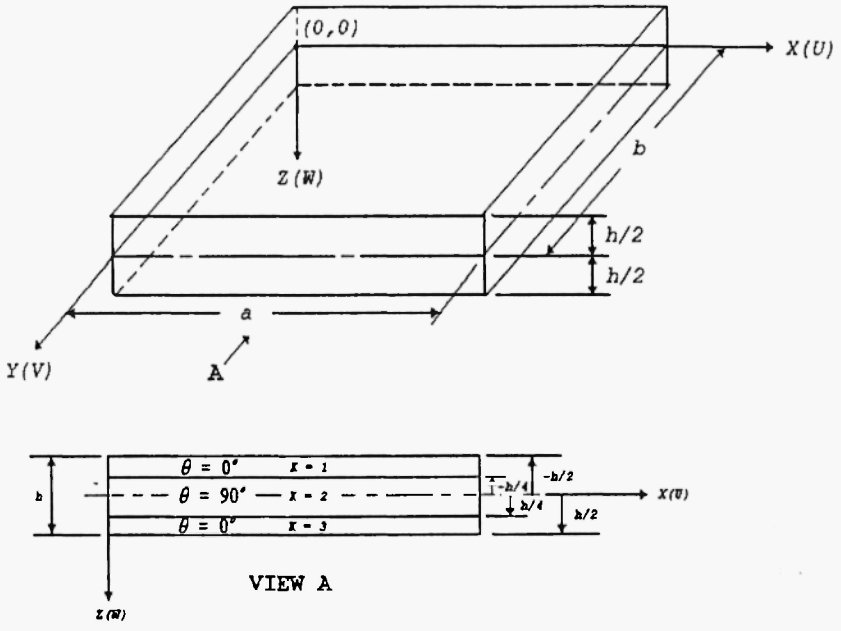

Fig. 1: A symmetric composite laminated plate.

each layer is assumed to possess a plane of elastic symmetry parallel to xy-plane. The origin of a Cartesian coordinate system is located within the central plane (x - y) with the z-axis being normal to this plane. It is assumed that the plate surfaces z= ±h /2 are subjected to surface tractions defined as

$$\tau_{xz}(x,y,\pm h/2,t)=0, \quad \tau_{yz}(x,y,\pm h/2,t)=0 \tag{1a}$$

$$\sigma_z(x,y,h/2,t)=q_1, \quad \sigma_z(x,y,-h/2,t)=q_2 \tag{1b}$$

where q_1 and q_2 are arbitrary functions of coordinates x, y, and z.

The stress and moment resultants can be defined, respectively, as

$$(N_x, N_y, N_{xy}, Q_x, Q_y) = \int_{-h/2}^{h/2} (\sigma_x, \sigma_y, \tau_x, \tau_{xz}, \tau_{yz})\, dz \tag{2a}$$

$$(M_x, M_y, M_{xy}) = \int_{-h/2}^{h/2} (\sigma_x, \sigma_y, \sigma_{xy})\, zdz \tag{2b}$$

Due to the presence of a plane of elastic symmetry, the constitutive relations for any given layer can be expressed as

$$\begin{bmatrix} \sigma_x \\ \sigma_y \\ \sigma_z \\ \tau_{xy} \end{bmatrix} = \begin{bmatrix} c_{11} & c_{12} & c_{13} & c_{16} \\ c_{21} & c_{22} & c_{23} & c_{26} \\ c_{31} & c_{32} & c_{33} & c_{36} \\ c_{61} & c_{62} & c_{63} & c_{66} \end{bmatrix} \begin{bmatrix} \varepsilon_x \\ \varepsilon_y \\ \varepsilon_z \\ \gamma_{xy} \end{bmatrix} \tag{3a}$$

$$\begin{bmatrix} \tau_{xy} \\ \tau_{xz} \end{bmatrix} = \begin{bmatrix} c_{44} & c_{45} \\ c_{54} & c_{55} \end{bmatrix} \begin{bmatrix} \gamma_{yz} \\ \gamma_{xz} \end{bmatrix} \tag{3b}$$

where c_{ij} are the components of the stiffness matrix and $\sigma_{(\,)}$, $\tau_{(\,)}$, $\varepsilon_{(\,)}$, and $\gamma_{(\,)}$ represent the engineering stress, shear stress, normal strain, and shear strain components, respectively.

For convenience, we employ compact notation to express the constitutive equations (3) in the form

$$\sigma_i = c_{ij}\, \varepsilon_j \qquad (i,j = 1,2,3,6) \tag{4}$$

where $\sigma_1 = \sigma_x$, $\sigma_2 = \sigma_y$, $\sigma_3 = \sigma_z$, $\sigma_6 = \tau_{xy}$ and the engineering strains ε_j are defined in an analogous manner. Combining (3) and (4), one can arrive at

$$\sigma_i = Q_{i\alpha}\, \varepsilon_\alpha + \frac{c_{i3}}{c_{33}}\, \sigma_3 \qquad (i = 1,2,3,6;\quad \alpha = 1,2,6) \tag{5}$$

in which $Q_{i\alpha}$ is defined as the plane stress reduced stiffness.

Further, one assumes the following displacement field

$$U = U^0(x,y,t) + z\psi_x(x,y,t) \tag{6a}$$

$$V = V^0(x,y,t) + z\psi_y(x,y,t) \tag{6b}$$

$$W = W^0(x,y,t) \tag{6c}$$

where U, V and W represent the displacement components in the x, y and z directions, respectively, while ψ_x and ψ_y are, respectively, the rotations of the normals to the mid-plane about the y and x axes. From equations (2), (5) and (6), and the assumption that the integrals associated with σ_2 are negligible and may be dropped, one obtains

$$\begin{bmatrix} N_x \\ N_y \\ N_{xy} \\ M_x \\ M_y \\ M_{xy} \end{bmatrix} = \begin{bmatrix} A_{11} & A_{12} & A_{16} & B_{11} & B_{12} & B_{16} \\ A_{21} & A_{22} & A_{26} & B_{21} & B_{22} & B_{26} \\ A_{61} & A_{62} & A_{66} & B_{61} & B_{62} & B_{66} \\ B_{11} & B_{12} & B_{16} & D_{11} & D_{12} & D_{16} \\ B_{21} & B_{22} & B_{26} & D_{12} & D_{22} & D_{26} \\ B_{61} & B_{62} & B_{66} & D_{61} & D_{62} & D_{66} \end{bmatrix} \begin{bmatrix} U^0_{,x} \\ V^0_{xy} \\ U^0_{,x} + V^0_{xy} \\ \psi_{x,x} \\ \psi_{y,y} \\ \psi_{x,x} + \psi_{y,y} \end{bmatrix} \tag{7a}$$

and

$$\begin{bmatrix} Q_x \\ Q_y \end{bmatrix} = k \begin{bmatrix} A_{44} & A_{45} \\ A_{54} & A_{55} \end{bmatrix} \begin{bmatrix} W_y + \psi_y \\ W_{,x} + \psi_x \end{bmatrix} \tag{7b}$$

where the differentiation is denoted by a comma, $( )_{ij} = ( )_{ji}$, and k, introduced in the expressions above for the transverse shear resultants, it is a material constant, representing a shear correction factor which depends on the analytical solution of the problem and the experimental results (e.g., Whitney & Pagano, 1970). In the set of equations (7),

$$(A_{ij}, B_{ij}, D_{ij}) = \int_{-h/2}^{h/2} Q_{ij}(1, z, z^2)\, dz \qquad (i,j = 1,2,6) \tag{8a}$$

$$A_{ij} = \int_{-h/2}^{h/2} c_{ij}\, dz \qquad (i,j = 4,5) \tag{8b}$$

The equations of motion in terms of stress and moment resultants are expressed as

$$N_{x,x} + N_{xy,y} = P\ddot{U}^0 + R\ddot{\psi}_x \tag{9a}$$

$$N_{xy,x} + N_{y,y} = P\ddot{V}^0 + R\ddot{\psi}_x \tag{9b}$$

$$Q_{x,x} + Q_{y,y} + q = PW \tag{9c}$$

$$M_{x,x} + M_{xy,y} - Q_x = R\ddot{U}^0 + I\ddot{\psi}_x \tag{9d}$$

$$M_{xy,x} + M_{y,y} - Q_y = R\ddot{V}^0 + I\ddot{\psi}_y \tag{9e}$$

with,

$$(P,R,I) = \int_{-h/2}^{h/2} \rho(1,z,z^2)dz \tag{10}$$

Further, by combining (7) and (9), one obtains the equations of motion in terms of the displacement components as (see Whitney & Pagano, 1970)

$$\begin{aligned} &A_{11}U^0_{,xx} + 2A_{16}U^0_{xy} + A_{66}U^0_{,yy} + A_{16}V^0_{xx} + (A_{12}+A_{66})V^0_{,xy} + A_{26}V^0_{,yy} + B_{11}\psi_{x,xx} \\ &+2B_{16}\psi_{x,xy} + B_{66}\psi_{x,yy} + B_{16}\psi_{y.xx} + (B_{12}+B_{66})\psi_{y\,xy} + B_{26}\psi_{y,yy} = P\ddot{U}^0 + R\ddot{\psi}_x \end{aligned} \tag{11a}$$

$$\begin{aligned} &A_{16}U^0_{,xx} + (A_{12}+A_{66})U^0_{,xy} + A_{26}U^0_{,yy} + A_{66}V^0_{xx} + 2A_{26}V^0_{,xy} + A_{22}V^0_{,yy} \\ &+ B_{16}\psi_{x,xx} + (B_{12}+b_{66})\psi_{x,xy} + B_{26}\psi_{x,yy} + B_{66}\psi_{y\,xx} \\ &+ 2B_{26}\psi_{y,xy} + B_{22}\psi_{y,yy} = P\ddot{V}^0 + R\ddot{\psi}_y \end{aligned} \tag{11b}$$

$$\begin{aligned} &k[A_{55}(\psi_{x,x} + \psi_{y,y}) + A_{45}(\psi_{x,y} + \psi_{y\,x} + 2W_{xy}) + A_{44} \\ &(\psi_{y,y} + W_{,yy})] + q = P\ddot{W} \end{aligned} \tag{11c}$$

$$\begin{aligned} &B_{11}U^0_{,xx} + 2B_{16} + U^0_{,xy} + B_{66}U^0_{yy} + B_{16}V^0_{,xx} + (B_{12}+N_{66})V^0_{xy} + B_{26}V^0_{,yy} \\ &+ D_{11}\psi_{x,xx} + 2D_{16}\psi_{x,xy} + D_{66}\psi_{x.vv} + D_{16}\psi_{y,xx} + (D_{12}+D_{66})\psi_{y\,xx} \\ &+ D_{26}\psi_{y,yy} - k[A_{55}(\psi_x + W_x) + A_{45}(\psi_y + W_y)] = R\ddot{U}^0 + I\ddot{\psi}_x \end{aligned} \tag{11d}$$

$$\begin{aligned} &B_{16}U^0_{,xx} + (B_{12}+B_{66})U^0_{,xy} + B_{26}U^0_{,yy} + B_{66}V^0_{,xx} + 2B_{26}V^0_{,xy} \\ &+ B_{22}V^0_{,yy} + D_{16}\psi_{x,xx} + (D_{12}+D_{66})\psi_{x,xy} + D_{26}\psi_{x,yy} + D_{66}\psi_{y\,xx} \\ &+12D_{26}\psi_{y\,yy} - k[A_{45}(\psi_x + W_x) + A_{44}(\psi_y + W_y)] = R\ddot{V}^0 + I\ddot{\psi}_y \end{aligned} \tag{11e}$$

In this, the value of the shear correction factor k was set, in the literature, as either 5/6, $\pi^2/12$ or 2/3. Ten and Sun (1983) advanced, however, that the value $\pi^2/12$, for the coefficient k, coincides satisfactorily with the experimental results.

2.2. Stress Wave Propagation

One assumes that the layers of the composite plate, Figure 1, are perfectly bonded together and that the plate is a symmetric cross-ply laminate, and it is simply supported all around on all edges. In this case, the following boundary conditions are seen to be applicable:

i) At x = 0 and x = a,

$$W = \psi_y = M_x = 0 \tag{12a}$$

$$V = N_x = 0 \tag{12b}$$

ii) At y = 0 and y = b,

$$W = \psi_x = M_y = 0 \tag{12c}$$

$$V = N_y = 0 \tag{12d}$$

From the above definition, and on the assumption that the symmetric cross-ply laminate could be treated as a homogeneous continuum of transversely isotropic material, one may further assume that

$$B_{ij} = 0, \quad R = 0, \quad A_{16} = A_{26} = D_{16} = D_{26} = A_5 = 0 \quad \text{and} \quad U, V = 0.$$

Accordingly, the five equations of motion (11), could be reduced to the following three equations with ψ_x, ψ_y, W are the only unknowns, i.e.,

$$k[A_{55}(\psi_{x,x} + W_{xx}) + A_{44}(\psi_{y\,y} + W_{yy})] + q = PW_{,tt} \tag{13a}$$

$$D_{11}\psi_{x,xx} + D_{66}\psi_{x,yy} + (D_{12} + D_{66})\psi_{y,xy} - kA_{55}(\psi_x + W_x) = I\psi_{x,tt} \tag{13b}$$

$$(D_{12} + D_{66})\psi_{x,xy} + D_{66}\psi_{y,xx} + D_{22}\dot{\psi}_{v,vv} - k\,A_{44}(\psi_y + W_{,y}) = I\psi_{y,tt} \tag{13c}$$

Following the Navier solution for plates subject to forced vibrations, the load distribution function q could be approximated by a double Fourier series. Therefore, one could obtain the general expression for the desired load distribution function as

$$q = \sum_{m,n=1}^{\infty} q_{mn}(t) \sin\frac{m\pi x}{a} \sin\frac{n\pi y}{b} \tag{14}$$

where the coefficients $q_{mn}(t)$ can be found by integrating the equation

$$q_{mn}(t) = \frac{4}{ab}\int_0^a\int_0^b q(x,y,t) \sin\frac{m\pi x}{a} \sin\frac{n\pi y}{b} \tag{15}$$

The general solutions for the above impact problem which satisfy the boundary conditions (12) can also be expressed, in a double Fourier series form, as

$$W(x,y,t) = \sum_{m,n=1}^{\infty} W_{mn}(t) \sin\frac{m\pi x}{a} \sin\frac{n\pi y}{b} \tag{16a}$$

$$\psi_x(x,y,t) = \sum_{m,n=1}^{\infty} X_{mn}(t) \cos\frac{m\pi x}{a} \sin\frac{n\pi y}{b} \tag{16b}$$

$$\psi_y(x,y,t) = \sum_{m,n=1}^{\infty} Y_{mn}(t) \sin\frac{m\pi x}{a} \cos\frac{n\pi y}{b} \tag{16c}$$

In order to apply the "*Correspondence Principle*" to solve this impact problem in viscoelasticity, it is necessary to use Fourier transform, i.e.,

$$f^F(x,y,\omega) = \int_{-\omega}^{\omega} f(x,y,t)\, e^{-i\omega t}\, dt \tag{17}$$

where the superscript $(\ )^F$ indicates the Fourier transform and ω is the Fourier parameter. By applying the Fourier transformation to equations (13), (14), and (16), one obtains the equations of motion in frequency-domain as

$$k[A_{55}(\psi^F_{x,x} + W^F_{,xx}) + A_{44}(\psi^F_{y,y} + W^F_{,yy})] + q^F = -\omega^2 P W^F \tag{18a}$$

$$D_{11}\psi^F_{x,xx} + D_{66}\psi^F_{x,yy} + (D_{12} + D_{66})\psi^F_{y,xy} - kA_{55}(\psi^F_x + W^F_x) = -\omega^2 I \psi^F_x \tag{18b}$$

$$(D_{11} + D_{66})\psi^F_{x,xy} + D_{66}\psi^F_{y,xx} + D_{22}\psi^F_{y,yy} - k A_{44}(\psi^F_y + W^F_y) = -\omega^2 I \psi^F_y \tag{18c}$$

Similarly, one obtains the double Fourier series of the already arrived-at general solutions as

$$W^F(x,y,\omega) = \sum_{m,n=1}^{\infty} W^F_{mn}(\omega) \sin\frac{m\pi x}{a} \sin\frac{n\pi y}{b} \tag{19a}$$

$$\psi^F_x(x,y,\omega) = \sum_{m,n=1}^{\infty} X^F_{mn}(\omega) \cos\frac{m\pi x}{a} \sin\frac{n\pi y}{b} \tag{19b}$$

$$\psi^F_y(x,y,\omega) = \sum_{m,n=1}^{\infty} Y^F_{mn}(\omega) \sin\frac{m\pi x}{a} \cos\frac{n\pi y}{b} \tag{19c}$$

and the Fourier transform of the impact loading distribution as

$$q^F(x,y,\omega) = \sum_{m,n=1}^{\infty} q^F_{mn}(\omega) \sin\frac{m\pi x}{a} \sin\frac{n\pi y}{b} \tag{20}$$

The Correspondence Principle is then adopted to transfer the above solutions from linear elasticity to linear viscoelasticity by simply replacing the elastic material parameters with their viscoelastic counterparts (e.g., Christensen, 1979 and Haddad, 1995, 2000), i.e. by taking

$$A_{ij} = A_{ij}^{*}(\omega) = A_{ij}^{*}, \quad D_{ij} = D_{i}^{*}(\omega) = D_{ij}^{*} \tag{21}$$

where A_{ij}^{*}, D_{ij}^{*} are complex frequency-dependent functions (Feng, 1999).

Substituting equations (19) and (20) into (18), then, by differentiation and proper manipulation, one obtains

$$W_{mn}^{F}(\omega) = \frac{a_4 a_5 a_7 - a_5^2 a_6}{a_1 a_4 a_5 a_7 - a_1 a_5^2 a_6 - a_2^2 a_5 a_7 + a_2 a_3 a_5^2 - a_3^2 a_4 a_5 + a_2 a_3 a_5 a_6} q_{mn}^{F}(\omega) \tag{22a}$$

$$X_{mn}^{F}(\omega) = \frac{a_2 a_5 a_7 - a_3 a_5^2}{a_2^2 a_5 a_7 - a_2 a_3 a_5^2 + a_3^2 a_4 a_5 - a_1 a_4 a_5 a_7 + a_1 a_5^2 a_6 - a_2 a_3 a_5 a_6} q_{mn}^{F}(\omega) \tag{22b}$$

$$Y_{mn}^{F}(\omega) = \frac{a_2 a_3 a_4 - a_2^2 a_6}{a_2 a_3^2 a_4 - a_2^2 a_3 a_6 + a_1 a_2 a_5 a_6 - a_2^2 a_3 a_5 + a_2^3 a_7 - a_1 a_2 a_4 a_7} q_{mn}^{F}(\omega) \tag{22c}$$

where

$$a_1 = kA_{55}^{*}\left(\frac{m^2\pi^2}{a^2}\right) + kA_{44}^{*}\left(\frac{n^2\pi^2}{b^2}\right) - \omega^2 P \tag{23a}$$

$$a_{21} = kA_{55}^{*}\left(\frac{m\pi}{a}\right); \qquad a_3 = kA_{44}^{*}\left(\frac{n\pi}{b}\right) \tag{23b}$$

$$a_4 = D_{11}^{*}\left(\frac{m^2\pi^2}{a^2}\right) + D_{66}^{*}\left(\frac{n^2\pi^2}{b^2}\right) + kA_{55}^{*} - \omega^2 I \tag{23c}$$

$$a_5 = (D_{12}^{*} + D_{66}^{*})\left(\frac{mn\pi^2}{a^2}\right); \qquad a_6 = (D_{11}^{*} + D_{66}^{*})\left(\frac{mn\pi^2}{b^2}\right) \tag{23d}$$

$$a_7 = D_{66}^{*}\left(\frac{m^2\pi^2}{a^2}\right) + D_{22}^{*}\left(\frac{m^2\pi^2}{b^2}\right) + kA_{44}^{*} - \omega^2 I \tag{23e}$$

2.3. Transient Wave Propagation under Impact Loading

The local rectangular impact load distribution is shown in Figure 2. The load is modelled as cosine-cosine distribution with respect to the space variables and sine distribution with respect to time. The centre of the load is considered to be located at coordinates (x_1, y_1) as shown in Figure 2. The function of the pertaining load distribution is expressed as (e.g., Prasad *et al.*, 1993)

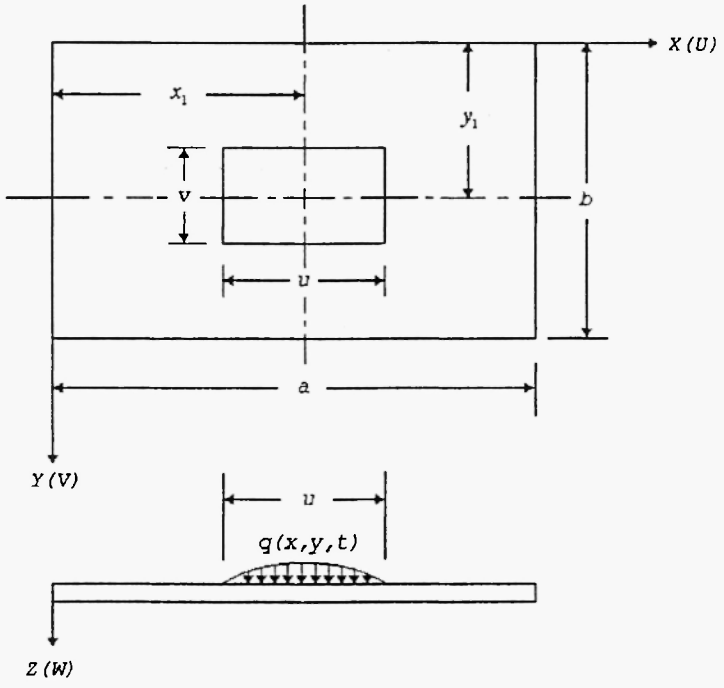

Fig. 2: Impact pressure distribution.

$$q = P_0 \cos\frac{\pi}{u}(x - x_1)\cos\frac{\pi}{v}(y - y_1)\sin\frac{\pi t}{\tau_0} \tag{24a}$$

$$\text{for } 0 < t < \tau_0,\ x_1 - \frac{u}{2} < x < x_1 + \frac{u}{2},\ y_1 - \frac{v}{2} < y \le y_1 + \frac{v}{2}$$

and,

$$q = P_0 \tag{24b}$$

$$\text{for } t > \tau_0;\ x < x_1 - \frac{u}{2},\ x > x_1 + \frac{u}{2};\ y < y_1 - \frac{v}{2},\ y > y_1 + \frac{v}{2}$$

By substituting equations (24) into Eqn. (15) and integrating, one obtains

$$q_{mn}(t) = \frac{16abuvP_0\cos\left(\frac{m\pi u}{2a}\right)\cos\left(\frac{m\pi v}{2b}\right)\sin\left(\frac{m\pi x}{a}\right)\sin\left(\frac{m\pi y}{b}\right)}{\pi^2(\mu + a)(\mu - a)(nv + b)(nv - b)}$$

$$\times \sin\left(\frac{\pi t}{\tau_0}\right) \tag{25a}$$

$$\text{for} \qquad mu \neq a,\ nv \neq b$$

$$q_{mn}(t) = 0 \qquad \text{for} \quad mu = a;\ n\nu = b \tag{25b}$$

The load distribution function can then be approximated by a double Fourier series as

$$q(x,y,t) = \frac{16abuvP_0}{\pi^2}\sin\left(\frac{\pi t}{\tau_0}\right)\sum_{m,n=1}^{\infty} \frac{\cos\left(\frac{m\pi u}{2a}\right)\cos\left(\frac{m\pi v}{2b}\right)\sin\left(\frac{m\pi x_1}{a}\right)\sin\left(\frac{m\pi y_1}{b}\right)}{(\mu+a)(\mu-a)(n\nu+b)(n\nu-b)} \tag{26a}$$

$$\text{for} \qquad mu \neq a;\ n\nu \neq b$$

$$q(x,y,t) = 0 \qquad \text{for} \quad mu = a;\ n\nu = b;\ t > \tau_0 \tag{26b}$$

In order to determine the solution for the viscoelastic dynamic system, Fourier transform is once again applied to transform the above load distribution function from time-domain to frequency-domain. In this context, by substituting equations (26) into equation (17), it follows that

$$q_F(x,y,\omega) = \frac{8abuvP_0\tau_0}{\pi^2}\left[\frac{1-\cos(\pi+\tau_0\omega)}{\pi+\tau_0\omega} + \frac{1-\cos(\pi-\tau_0\omega)}{\pi-\tau_0\omega} + i\left(\frac{\sin(\pi+\tau_0\omega)}{\pi+\tau_0\omega} - \frac{\sin(\pi-\tau_0\omega)}{\pi-\tau_0\omega}\right)\right] \tag{27a}$$

$$\sum_{m,n=1}^{\infty} \frac{\cos\left(\frac{m\pi u}{2a}\right)\cos\left(\frac{m\pi v}{2b}\right)\sin\left(\frac{m\pi x_1}{a}\right)\sin\left(\frac{n\pi y_1}{b}\right)\sin\left(\frac{m\pi x}{a}\right)\sin\left(\frac{n\pi y}{b}\right)}{(\mu+a)(\mu-a)(n\nu+b)(n\nu-b)}$$

$$\text{for} \qquad mu \neq a,\ n\nu \neq b;\ \omega\,\tau_0 \neq \pi$$

and,

$$q^F(x,y,\omega) = 0 \qquad \text{for} \quad mu = a,\ n\nu = b,\ \omega\,\tau_0 = \pi \tag{27b}$$

From equation (20), one can determine the complex coefficient $q^F_{mn}(\omega)$ as

$$q_{mn}^{F}(\omega) = \frac{8abuvP_0\tau_0\cos\left(\frac{m\pi u}{2a}\right)\cos\left(\frac{m\pi v}{2b}\right)\sin\left(\frac{m\pi x_1}{a}\right)\sin\left(\frac{n\pi y_1}{b}\right)}{(\mu+a)(\mu-a)(nv+b)(nv-b)}$$
$$\left[\frac{1-\cos(\pi+\tau_0\omega)}{\pi+\tau_0\omega}+\frac{1-\cos(\pi-\tau_0\omega)}{\pi-\tau_0\omega}+i\left(\frac{\sin(\pi+\tau_0\omega)}{\pi+\tau_0\omega}-\frac{\sin(\pi-\tau_0\omega)}{\pi-\tau_0\omega}\right)\right] \quad (28a)$$

for $mu \neq a, nv \neq b; \omega\tau_0 \neq \pi$

and,

$$q^{F}(\omega) = 0 \quad \text{for} \quad mu = a, nv = b, \omega\tau_0 = \pi \quad (28b)$$

In order to obtain the required transient wave solutions, one combines (28) with (22) and (19), to arrive first at the solution in the frequency domain. Then, by applying the viscoelastic parameters A_{44}^{*}, A_{55}^{*}, D_{11}^{*}, D_{12}^{*}, D_{22}^{*} and D_{66}^{*} as defined in (Feng, 1999), the Fast Fourier Transform (FFT) can be employed in order to numerically transform these solutions from frequency-domain to time-domain.

3. NUMERICAL RESULTS AND DISCUSSION

As mentioned in the foregoing, the dynamic solutions, obtained in the frequency-domain, are required to be inverted into the time-domain by utilizing, for instance, Fourier transform. Due to the complexity of the obtained dynamic solutions, however, the discrete Fourier transform would be an appropriate choice. Normally, the discrete Fourier transform is expressed in pair as follows,

$$G\left(\frac{n}{NT}\right) = \sum_{k=0}^{N-1} g(kT)e^{-i2w\pi nk/N} \qquad n = 0.1, \ldots, N-1 \quad (29)$$

$$g(kT) = \frac{1}{N}\sum_{n=0}^{N-1} G\left(\frac{n}{NT}\right) e^{-i2w\pi nk/N} \qquad K = 0.1, \ldots, N-1 \quad (30)$$

where N is the total sampling number, T is sampling interval, and G (.) and g (.) represent the desired function in the frequency and time domain, respectively.

In engineering computation, the reason for the wide use of Fourier transform is due to its capability to allow one to examine a function from the perspective of both time and frequency domains. The time and effort are further eased due to the development of the discrete Fourier transform which permits one to analyse behaviour of the function in a numeric fashion. Due to the large number of sampling involved in the dynamic analysis, the Fast Fourier Transform (FFT) is adopted in the present work.

An essential requirement of a FFT operation (e.g., Brigham, 1988) is the determination of the total

sampling number N and the sampling interval T, which directly affect the results of the FFT computation (*see* Appendix A for the FFT computer program flowchart used in the present analysis).

With reference to Figures 1 and 2, the dimensions of the composite laminate are set as a = 20.0 inches, b = 10.0 inches and h = 1.0 inches with each lamina being composed of an epoxy matrix, with embedded-in glass fibres. The impact is assumed to be the unit load p = 1.0, with a contact duration $\tau_0 = 1 \times 10^{-6}$ sec, located at the centre of the plate, at $x_1 = 10.0$ inches and $y_1 = 5.0$ inches, with the loading area being a square, i.e., u = v = 0.1 inches. It is further assumed that the matrix material behaves as a linear viscoelastic material, whereby the real part of its complex modulus is represented by (e.g., Christensen, 1979)

$$E_{mr} = 1158\,(1 + 100f)^{0.1} \tag{31}$$

The damping factor of the viscoelastic matrix is assumed to be constant. It is set to assume the values of 0.05 and 0.15 for comparison. The embedded-in glass fibres are assumed to be elastic in response. Glass fibres with limited viscoelastic response are also considered for comparison. The damping factor for the latter is set as 0.0014. The effects of microstructural parameters, such as fibre volume fraction and fibre- aspect-ratio on the impact behaviour of the composite laminate are examined. Values of other material properties, i.e., elastic modulus, shear modulus, shear damping factor, Poisson's ratio and specific gravity, are set as shown in Table 1 for both the fibre and matrix. The presented values of these properties are assumed to be constant for the ease of calculation. Based on the analysis conducted by Prasad *et al.* (1993), the value of the shear parameter k, mentioned in the foregoing, is set as $\pi^2/12$ (see, also, Ten and Sun, 1983). The total sampling number N and the sample time-interval T for the pertaining FFT algorithm are set, respectively, as

Table 1

Static Properties of Scotchply 1002 Matrix Epoxy and E-glass Fibres at Room Temperature, after Gibson *et al.* (1976).

Material Properties - GPa (10^6 Psi)	Epoxy	E-glass
Young's modulus - GPa (10^6 Psi)	3.79 (0.55)	72.4 (10.5)
Shear Modulus	1.38 (0.2)	30.3 (4.4)
Damping Factor	0.015	0.0014
Shear Damping Factor	0.018	0.0014
Poisson's Ratio	0.36	0.2
Specific Gravity (g)	1.23	2.54

8192 and 2×10^{-6} sec. (Feng, 1999). For the purpose of limiting the length of this paper, only displacements along the z-axis are graphically illustrated.

Figure 3 shows both the real and imaginary parts of the displacement in the frequency-domain as well as their inverted Fourier transform in the time-domain. The significant attenuation, due to the viscoelastic nature of this kind of materials, is observed in this Figure.

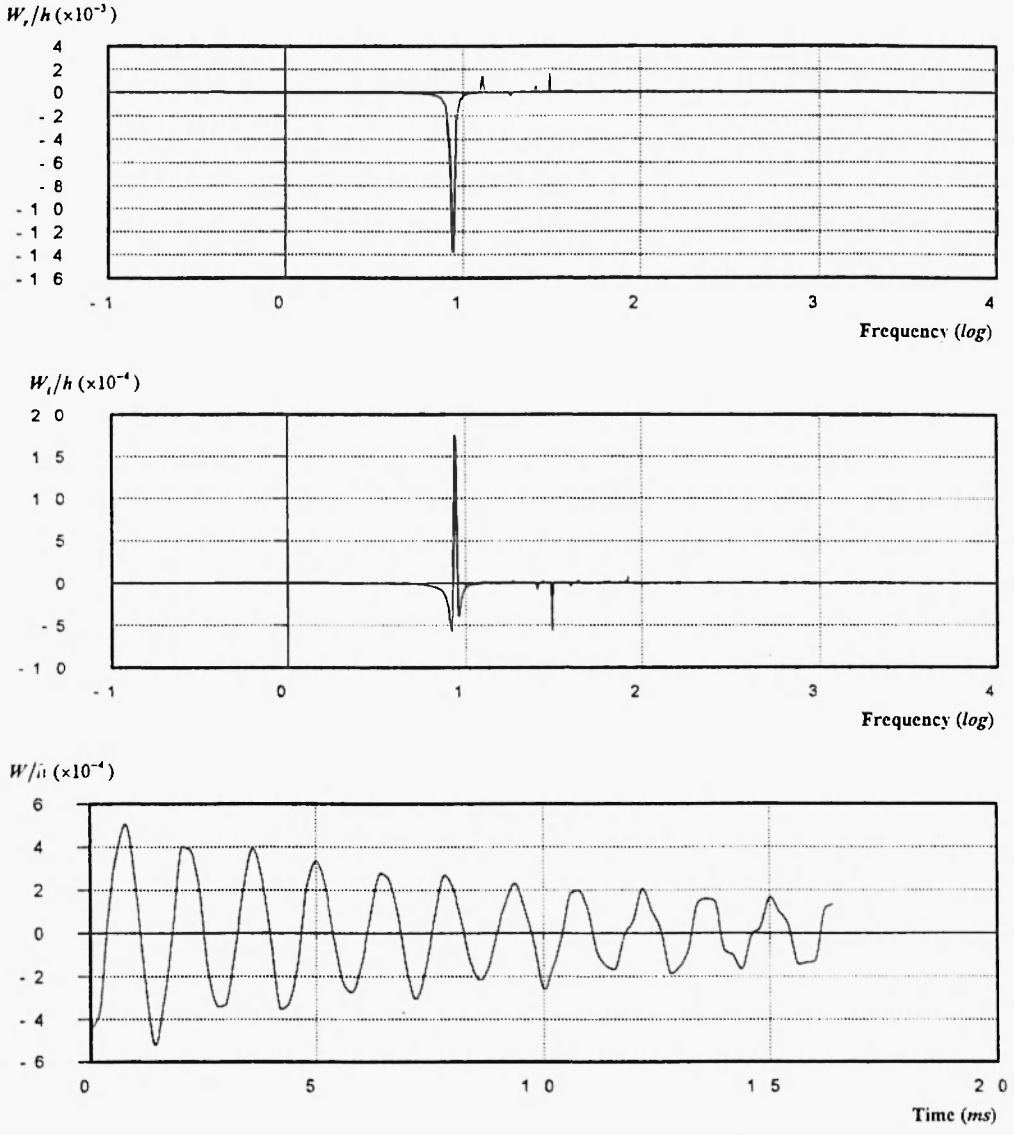

Fig. 3: Illustration of Fourier Transformation. The top two figures show the wave propagation solutions in their frequency-domain which can be transformed by using FFT algorithm into time-domain as shown in the bottom figure.

The effect of the damping factor of the matrix material on the impact response of composite laminates is presented in Figure 4. In this Figure, one observes that, under the same loading condition, a composite-laminate with matrix of a higher damping factor produces a much smaller amplitude of the waveform-displacement when compared with a laminate of a lower damping factor. It is obvious that the waveform of the laminate with a matrix of a lower damping factor is not as smooth as the one with a matrix of a higher damping factor, and, thus, is more complex to analyse. One, also, observes, in Figure 4, that the laminate with a matrix of lower damping factor exhibits a higher attenuation rate in the first 3 to 4 *ms*. The attenuation seems to slow down after the first 4 *ms* and the amplitude of the response waveform appears to be constant after the first 12 *ms*. For the laminate with a matrix of higher damping factor, attenuation is observed to be consistent throughout the entire time scale.

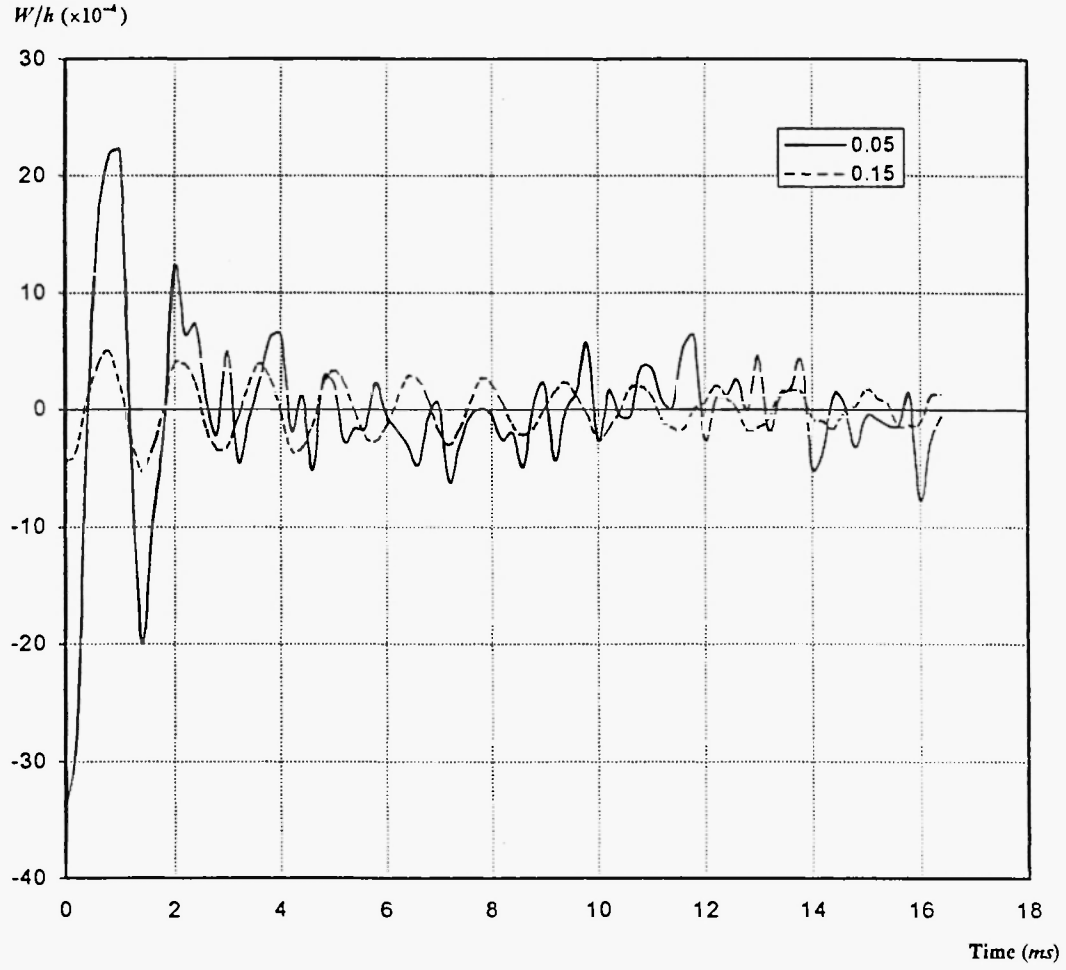

Fig. 4: Impact response of composite laminates with matrices have different damping factors, i.e., 0.5 (solid line) and 0.15 (dashed line). Other material properties are set as: the real modulus of matrix is $E_{mr} = 1158\,(1+100f)^{0.1}$, with f as frequency, the real modulus of glass fibre (continuous) is 72.4 GPa, fibre volume fraction is 60%, and damping factor of the fibre is 0.0014.

The effect of viscoelasticity of the fibre material, on wave propagation in the dealt-with class of composite laminate, is illustrated in Figure 5, whereby both elastic and viscoelastic glass fibre materials are considered under the same loading condition. In Figure 5, one observes that there is not much difference in effect between the considered elastic and viscoelastic fibres except in the first 1 - 1.5 *ms* time duration. This is due to the extremely low value of the damping factor of the considered glass fibre, which may be considered, for the ease of calculations, as a linear elastic material. The attenuation of the waveform, in both cases, is thus due the viscoelastic matrix.

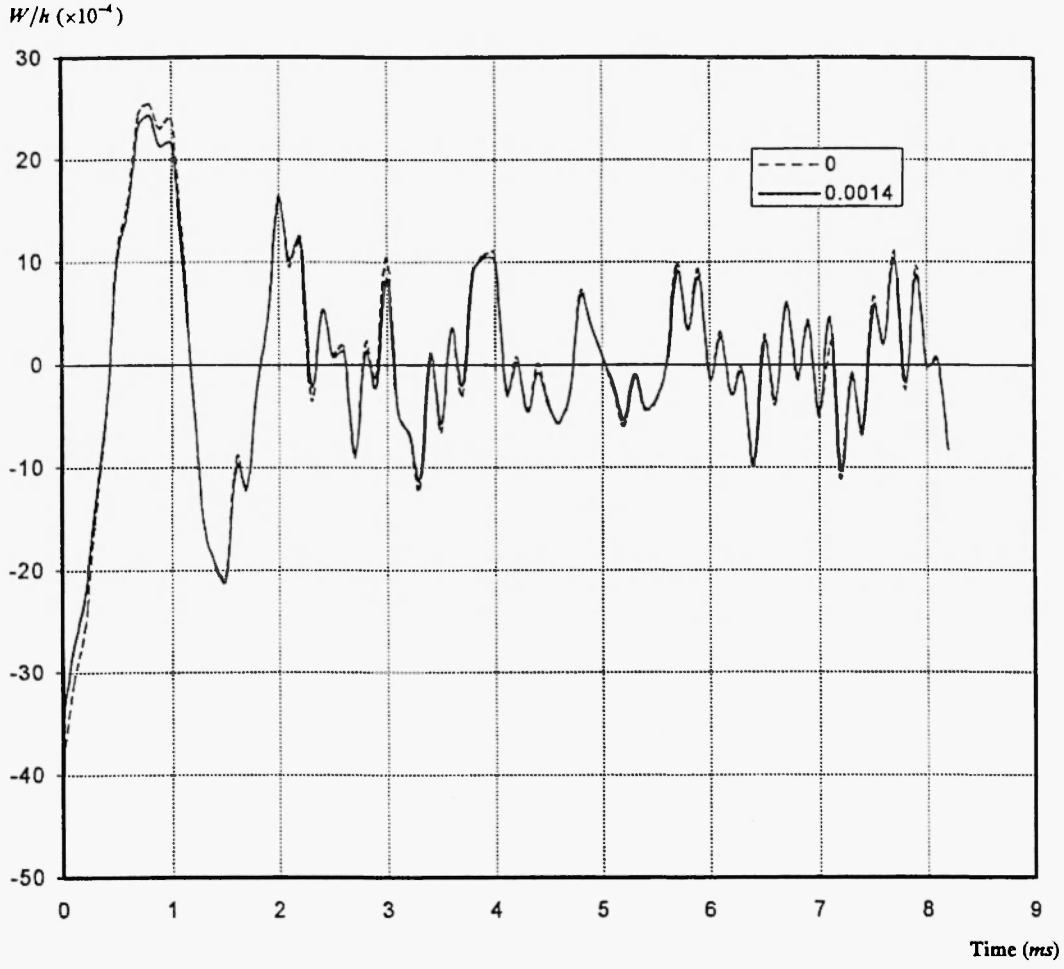

Fig. 5: Impact response of composite laminates with elastic and viscoelastic fibres, i.e., fibre damping factors as 0.0014 (solid line) and 0.00 (dashed line). Other material properties are set as: the real modulus of glass fibre (continuous) is 72.4 GPa, fibre volume fraction is 60%, the real modulus of the matrix is $E_{mr} = 1158\ (1 + 100f)^{0.1}$, with f as frequency, and damping factor of the matrix is 0.05.

Figures 6 and 7 present the effect of fibre volume fraction on the impact response of the laminate with a matrix damping factor of 0.15 and 0.05, respectively. Apparently, the initial amplitude of response waveform of a composite laminate of a higher fibre volume fraction is much more significant as compared with that of a smaller fibre volume fraction. This observation ascertains that the viscoelasticity of the laminate increases as the fibre volume fraction, of the class of the considered fibres, decreases. The delayed phase response of a composite laminate with a lower fibre volume fraction is also observed when compared with that pertaining to a higher fibre volume fraction laminate. This may be attributed to a corresponding change in the transverse properties of the laminate.

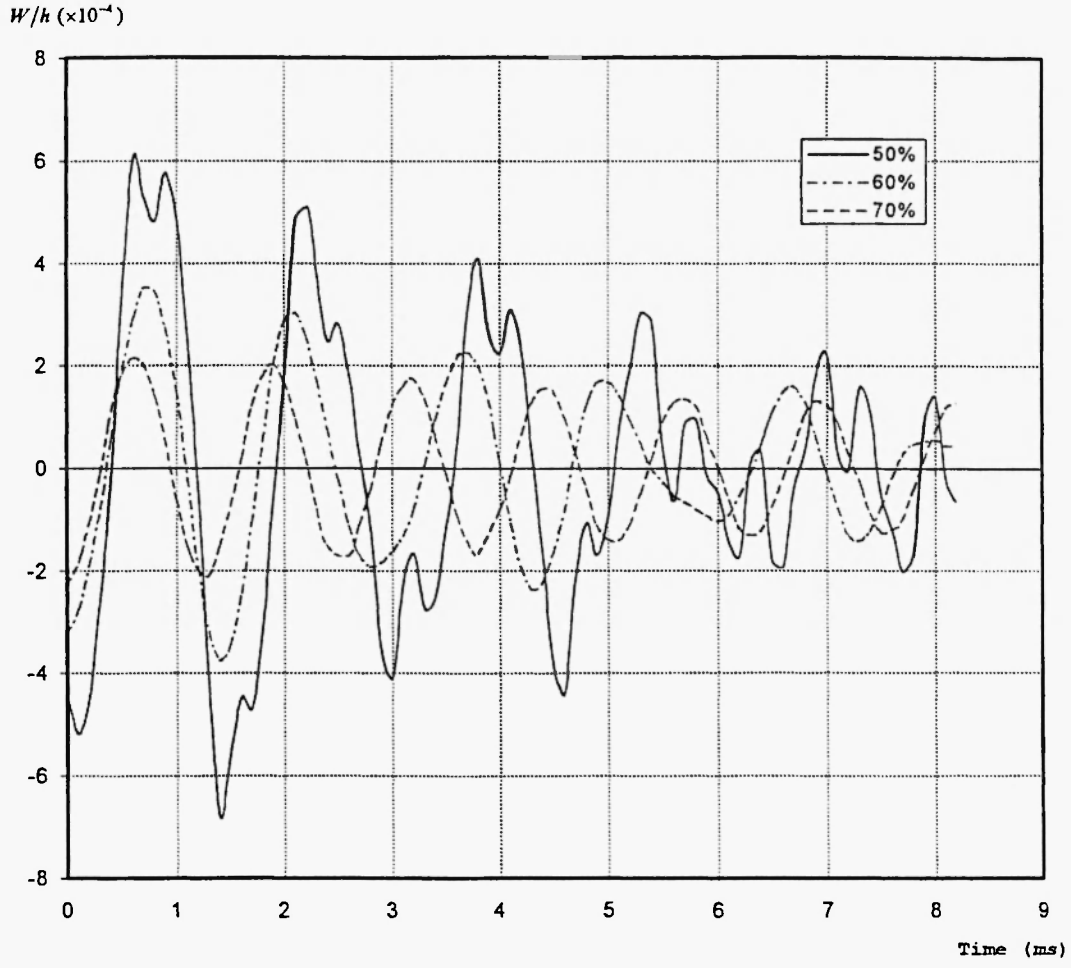

Fig. 6: Impact response of composite laminates with various fibre volume fractions, i.e. 50% (solid line), 60% (dash-dotted line) and 70% (dashed line). Other material properties are set as: the real modulus of glass fibre (continuous) is 72.4 GPa, fibre damping factor is 0.0014, the real modulus of the matrix is $E_{mr} = 1158\ (1+100f)^{0.1}$, with f as frequency, and damping factor of the matrix is 0.15.

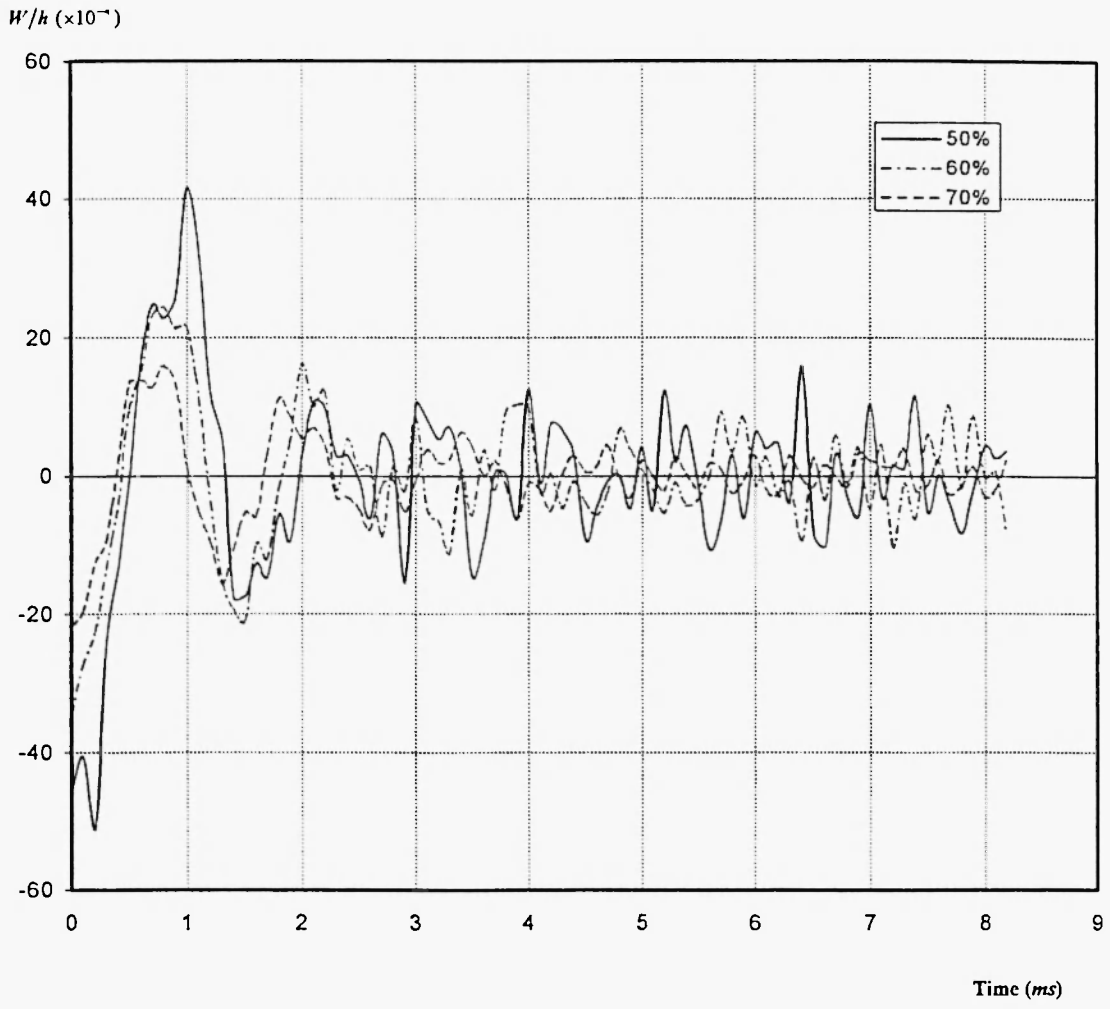

Fig. 7: Impact response of composite laminates with various fibre volume fractions, i.e. 50% (solid line), 60% (dash-dotted line) and 70% (dashed line). Other material properties are set as: the real modulus of glass fibre (continuous is 72.4 GPa, fibre damping factor is 0.0014, the real modulus of the matrix is $E_{mr} = 1158\,(1+100f)^{0.1}$, with f as frequency, and damping factor of the matrix is 0.05.

Due to the high volume of discontinuous fibre reinforced composite applications in automotive and aerospace industries and their superior damping capacities compared to continuous fibre reinforced composites, it is equally important to examine the effect of discontinuous fibre-reinforcement on the dynamic response of the composite laminate under impact loading. The effect of discontinuous fibre reinforcement on the mechanical properties under static loading was analysed in previous work by the authors (e.g., Haddad and Feng, 2000 and Feng, 1999); see, also Gibson and Yau (1980), Gibson *et al.* (1982), Sun *et al.* (1985) and Suarez *et al.* (1986). The observation made by Cox (1952) shows that, for fibre-reinforced composite

materials, the reduction of the effective longitudinal modulus due to the load transfer from fibre to fibre is important only if the fibre-aspect-ratio is less than 100. In this context, Figures 8 and 9 compare the wave propagation pattern of composite laminae with continuous *vs.* discontinuous fibre-reinforcement, with the matrix damping factor is set as 0.15 and 0.05, respectively, for comparison. For the composite laminate with a matrix of low damping matrix, the response waveform fits well with the observation made by Cox (1952) that the discontinuous fibre- reinforced laminate with a fibre-aspect-ratio larger than 100 can be treated as a continuous fibre-reinforced laminate. For the laminate with a higher damping matrix, there is, however, a slight difference between the two pertaining results.

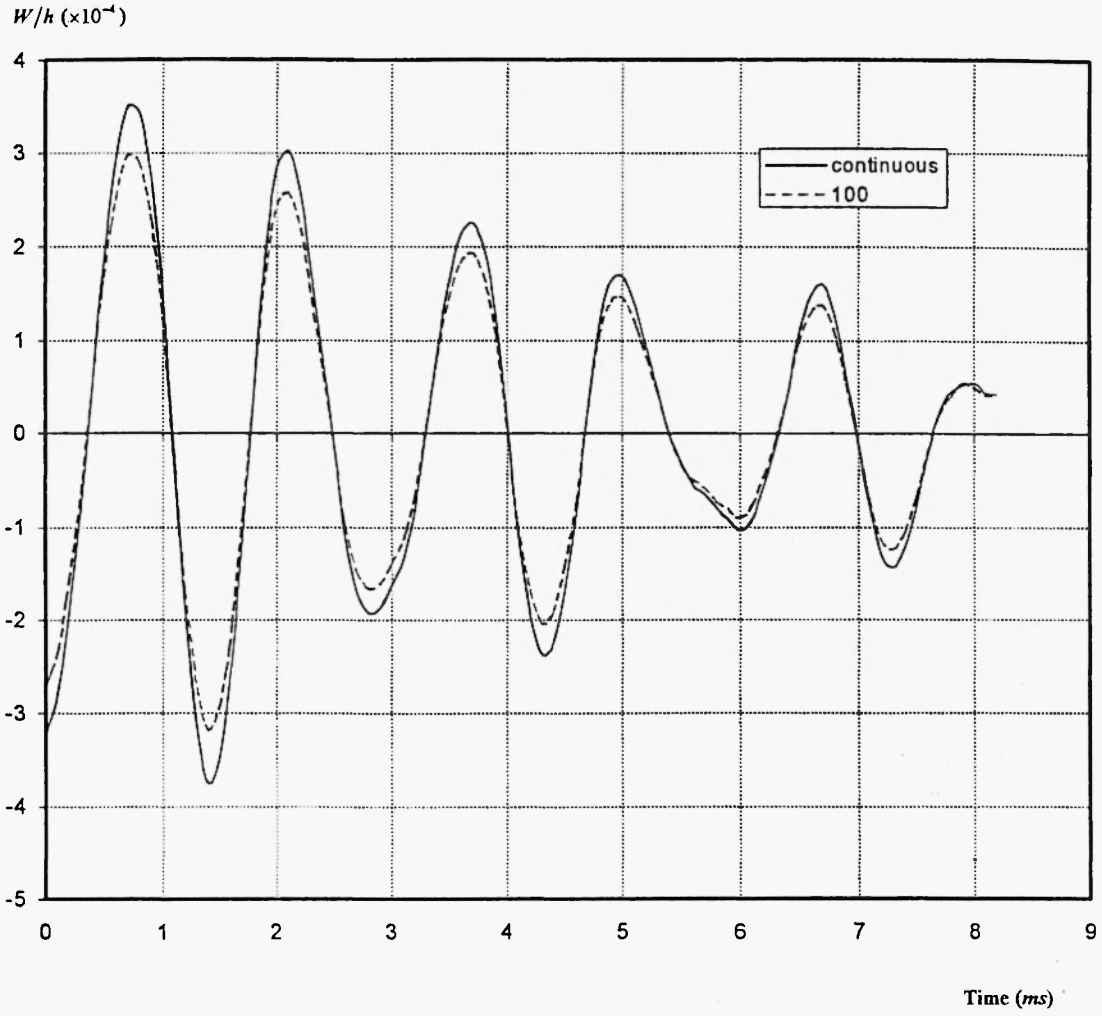

Fig. 8: Impact response of composite laminates with various fibre aspect ratios, i.e. continuous (solid line), and 100 (dash-dotted line). Other material properties are set as: the real modulus of glass fibre is 72.4 GPa, fibre damping factor is 0.0014, fibre volume fraction is 60%, the real modulus of the matrix is $E_{mr} = 1158\,(1+100f)^{0.1}$, with f as frequency, and damping factor of the matrix is 0.15.

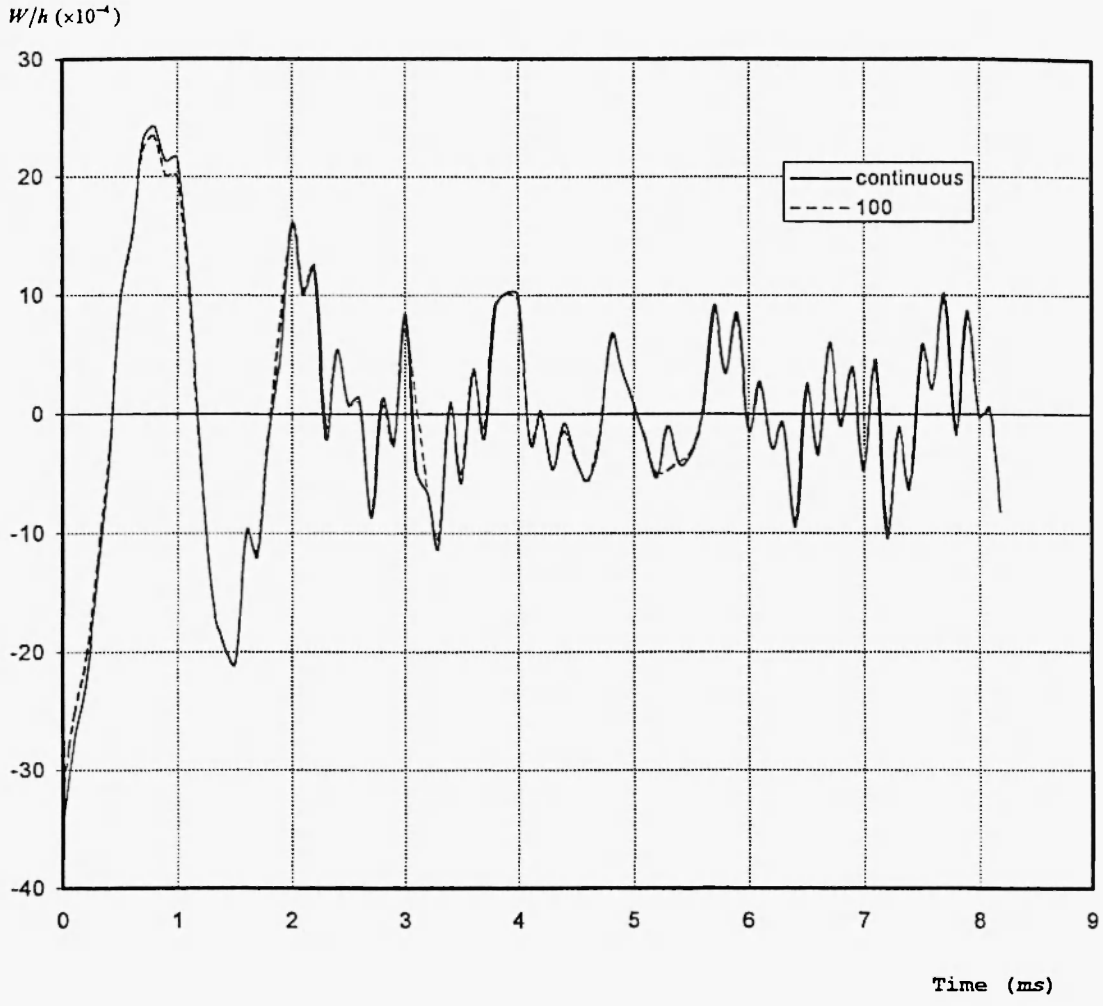

Fig. 9: Impact response of composite laminates with various fibre aspect ratios, i.e. continuous (solid line), and 100 (dash-dotted line). Other material properties are set as: the real modulus of glass fibre is 72.4 GPa, fibre damping factor is 0.0014, fibre volume fraction is 60%, the real modulus of the matrix is $E_{mr} = 1158\,(1+100f)^{0.1}$, with f as frequency, and damping factor of the matrix is 0.05.

Figures 10 and 11 compare the effect of different fibre-aspect-ratio on the dynamic response under the same impact loading for the cases of laminates with both low and high damping matrices (i.e., damping factor of 0.05 and 0.15, respectively). The same trend could be found from both figures that the amplitude of response waveform decreases with the decrease of the fibre-aspect-ratio, which agrees well with the observations made earlier by the authors; *see* Haddad and Feng (2000) and Feng (1999). It is generally agreed upon that the change of fibre volume fraction results in a corresponding change in the overall mechanical properties of the considered composite, i.e., including changes in the longitudinal as well as

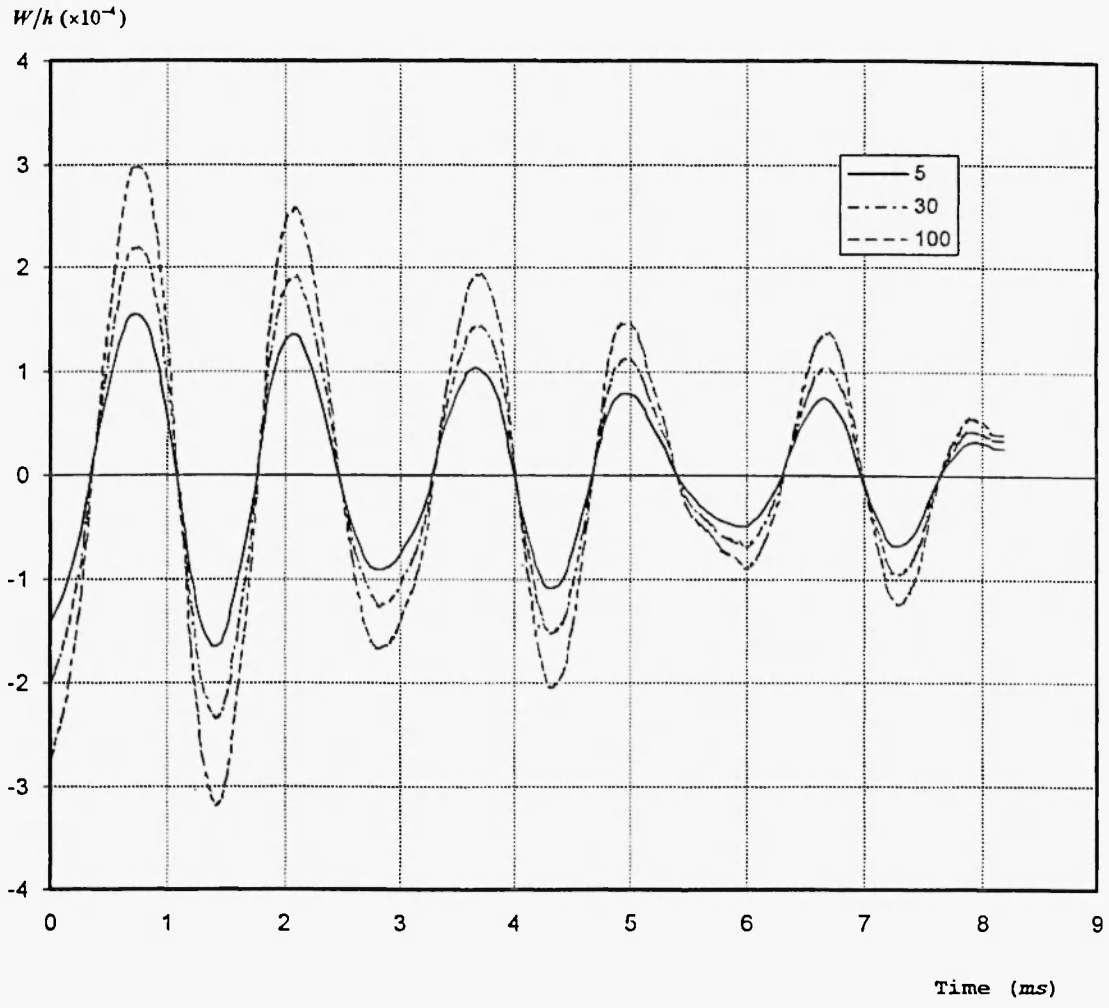

Fig. 10: Impact response of composite laminates with various fibre aspect ratios, i.e. 5 (solid line), 30 (dash-dotted line), and 100 (dashed line). Other material properties are set as: the real modulus of glass fibre is 72.4 GPa, fibre damping factor is 0.0014, fibre volume fraction is 60%, the real modulus of the matrix is $E_{mr} = 1158\ (1+100f)^{0.1}$, with f as frequency, and damping factor of the matrix is 0.15.

transverse properties. On the other hand, a change in the fibre-aspect-ratio may only change material properties at longitudinal (fibre) direction. Thus, with reference to Figures 6 and 7, it is interesting to note that, due to their different relationship with material damping properties and stiffness, fibre-aspect-ratio has a different effect on the impact response of the composite laminate if compared with fibre volume fraction. It is also interesting to observe that the phase of the response waveform does not vary in correspondence to the change of fibre-aspect-ratio (Figures 10 and 11).

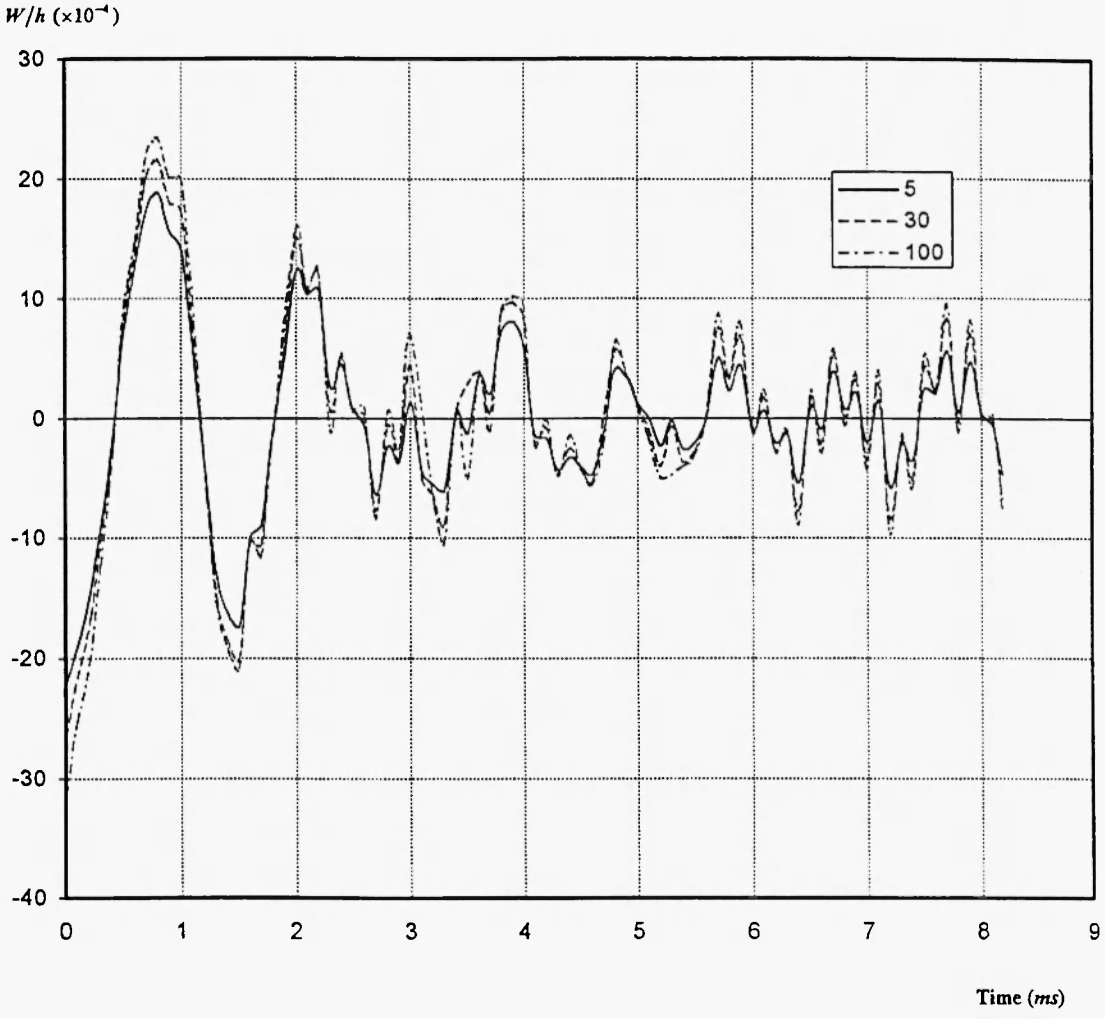

Fig. 11: Impact response of composite laminates with various fibre aspect ratios, i.e. 5 (solid line), 30 (dash-dotted line), and 100 (dashed line). Other material properties are set as: the real modulus of glass fibre is 72.4 Gpa, fibre damping factor is 0.0014, fibre volume fraction is 60%, the real modulus of the matrix is $E_{mr} = 1158\ (1+100\ f)^{0.1}$, with f as frequency, and damping factor of the matrix is 0.05.

4. CONCLUSIONS

(1) The anisotropy and the viscoelastic nature of composite laminates make wave propagation analysis much more complex as compared to their isotropic and elastic counterparts. The "First Shear Deformation Theory" (FSDT), Whitney and Pagano (1970), is adopted, and appears to work well in the presented analysis. During the course of the analysis, the "Navier Solution" for plates under forced vibrations and "Fourier Transformation" are utilised to transfer the equations of motion from time-domain to frequency-domain. Then, the "Correspondence Principle" is applied to solve the impact problem in linear viscoelasticity. Finally, the Fast Fourier Transformation (FFT) is employed to inverse these solutions from frequency-domain into time-domain.

(2) For a given E-glass/Epoxy laminated composite, the matrix material makes a major contribution to the attenuation of stress waves. In this context, it is evident that transit wave propagation, in polymeric composite systems, must be examined within the scope of Viscoelasticity.

(3) The resulted transit wave propagation has been further explored in relation to the properties of the microstructural constituents. The attenuation of the laminate with a lower fibre volume fraction is much more significant than the one with a higher fibre volume fraction. The same phenomenon is also identified for the laminate with a lower fibre-aspect-ratio compared with the one with a higher fibre-aspect-ratio. These results are in agreement with the observations made earlier by the authors (e.g., Haddad and Feng, 2000 and Feng, 1999) that discontinuous fibre-reinforced composites have a damping property superior than that of the corresponding continuous-fibre composite and that composites with a lower fibre volume fraction have superior energy absorbing capability compared with the ones with a higher fibre volume fraction. These results further demonstrate that in order to increase the damping, it is necessary to sacrifice the stiffness, and vice versa. Such a trade-offs requires a careful examination, but, meantime, it provides flexibility in the course of designing a laminated composite with discontinuous fibre-reinforcement.

5. REFERENCES

Abrate, S. (1991) Impact on laminated composite materials, *Applied Mechanics Review* **44** (4), 155-90.

Abrate, S. (1994) Impact on laminated composite materials, *Applied Mechanics Review* **47** (11), 517-44.

Brigham, E. Oran, (1988) *The Fast Fourier Transformation & its Applications*, Prentice Hall, Englewood Cliffs, New Jersey.

Burtin, C. and Hamelin, P. (1986) Effect of viscoelastic characteristics of polymers for a composite behaviour under dynamic and impact loading, in *Mechanical Behaviour of Composites and Laminates*, edited by W.A. Green and M. Micunovic, European Mechanics Colloquium 214, Kupari, Croatia, pp. 32-44.

Cederbaum, G. and Aboudi, J. (1989) Dynamic response of viscoelastic laminated plates, *Journal of Sound and Vibration* **133** (2), 225-38.

Christensen, R.M. (1979) *Mechanics of Composite Materials*, Wiley, New York.

Cox, H.L. (1952) The elasticity and strength of paper and other fibrous materials, *British Journal of Applied Physics* **3**, 72-84.

Daniel, I.M., Liber, T. and LaBedz, R.H. (1979) Wave propagation in transversely impacted composite laminates, *Experimental Mechanics* **1**, 9-16.

Feng, J. (1999) *On the Viscoelastic Response of Laminated Composites*, M.A. Sc. Thesis, Dept. of Mechanical Engineering , University of Ottawa, Canada.

Gibson, R.F., Chaturvedi, S.K. and Sun, C.T. (1982) Complex moduli of aligned discontinuous fibre-reinforced polymer composites, *Journal of Materials Science* **17**, 3499-509.

Gibson, R.F. and Plunkett, R. (1976) Dynamic mechanical behaviour of fibre reinforced composites: Measurement and Analysis, *Journal of Composite Materials* **10**, 325-41.

Gibson, R.F. and Yau, A. (1980) Complex moduli of chopped fibre and continuous fibre composites: Comparison of measurements with estimated bounds, *Journal of Composite Materials* **14**, 155-67.

Green, W.A. and Baylis, E.R. (1988) The Propagation of Impact Stress Waves in Anisotropic Fibre Reinforced laminates, *Wave Propagation in Structural Composites* (ASME, Applied Mechanics Division), Vol. 90, Publ by ASME, New York, USA, pp. 53-68.

Haddad, Y.M. (1995) *Viscoelasticity of Engineering Materials*, Kluwer, Dordrecht.

Haddad, Y.M. (2000) *Mechanical Behaviour of Engineering Materials*, Vol. I and II. Kluwer, Dordrecht.

Haddad, Y.M. and Feng, J. (2000) On the trade-off between damping and stiffness in the design of discontinuous fiber-reinforced composites, Mesomechanics 2000, Xi'ian, China, June 13-16, 2000.

Kam, T.Y. and Chang, W.J. (1995) Impact analysis of shear deformable laminated composite plates, *Journal of Energy Resources Technology* **117**, 219-27.

Kim, B.S. and Moon, F.C. (1977) Impact induced stress waves in an anisotropic plate, *AIAA Journal* **17(10)**, 1126-33.

Kolsky, H. (1963) *Stress Waves in Solids*, Dover Publications, Inc., USA.

Ma, C.C. and Huang, K.H. (1995) Wave propagation in layered elastic media for antiplane deformation, *Journal of Solids Structures* **32** (5), 665-78.

Mindlin, R.D. (1961) High frequency vibrations of crystal plates, *Quarterly of Applied Mathematics* **19(1)**, 51-61.

Mindlin, R.D. and Medick, M.A. (1959) Extensional vibration of elastic plates, *Journal of Applied Mechanics* **26**, 561-9.

Moon, F.C. (1972) Wave surfaces due to impact on anisotropic plates, *Journal of Composite Materials* 6, 62-79.

Moon, F.C. (1973a) One-dimensional transient waves in anisotropic plates, *Journal of Applied Mechanics* **6**, 485- 90.

Moon, F.C. (1973b) Stress wave calculations in composite plates using the Fast Fourier Transform, *Computers and Structures* **3**, 1195-204.

Moon, F.C. (1975) Wave propagation and impact in composite materials, in *Composite Materials,* Vol. 7, Part I, edited by C.C. Chamis, pp. 259-332.

Prasad, C.B., Ambur, D.R. and Stames, J.H. Jr. (1993) Response of laminated composite plates to low-speed impact by air-gun-propelled and dropped-weight impactors", AIAA-93-1402-CP, *Collection of Papers of AIAA*, Part 2, pp. 887-900.

Suarez, S.A., Gibson, R.F., Sun, C.T. and Chaturvedi, S.K. (1986) The influence of fibre length and fibre orientation on damping and stiffness of polymer composite materials, *Experimental Mechanical* **6**, 175-84.

Sun, C.T., Gibson, R.F. and Chaturvedi, S.K. (1985) Internal materials damping of polymer matrix composites under off-axis loading, *Journal of Materials Science* **20**, 2575-85.

Sun, C.T. and Lai, R.Y.S. (1974) Exact and approximate analyses of transient wave propagation in an anisotropic plate, *AIAA Journal* **10**, 1415-17.

Sun, C.T. and Wang, T. (1986) Impact wave response and failure in composite laminates, in *Mechanical Behaviour of Composites and Laminates*, edited by W.A. Green and M. Micunovic, European Mechanics Colloquium 214, Kupari, Croatia, pp. 19-31.

Ten, T.M. and Sun, C.T. (1983) *Impact Wave Propagation of Fibre Reinforced Composite Laminates*, PhD dissertation, Department of Mechanical Engineering, Purdue University, USA.

Whitney, J.M. and Pagano, N.J. (1970) Shear deformation in heterogeneous anisotropic plates, *Journal of Applied Mechanics* **12**, 1031-6.

ACKNOWLEDGMENTS

The operating research grant from NSERC - Natural Sciences and Engineering Council of Canada, to the second author, is sincerely acknowledged. The second author wishes also to express his gratitude for the financial grant from the Ontario Ministry of Colleges and Universities within the scope of the Ontario-Quebec Exchange Program.

Appendix A

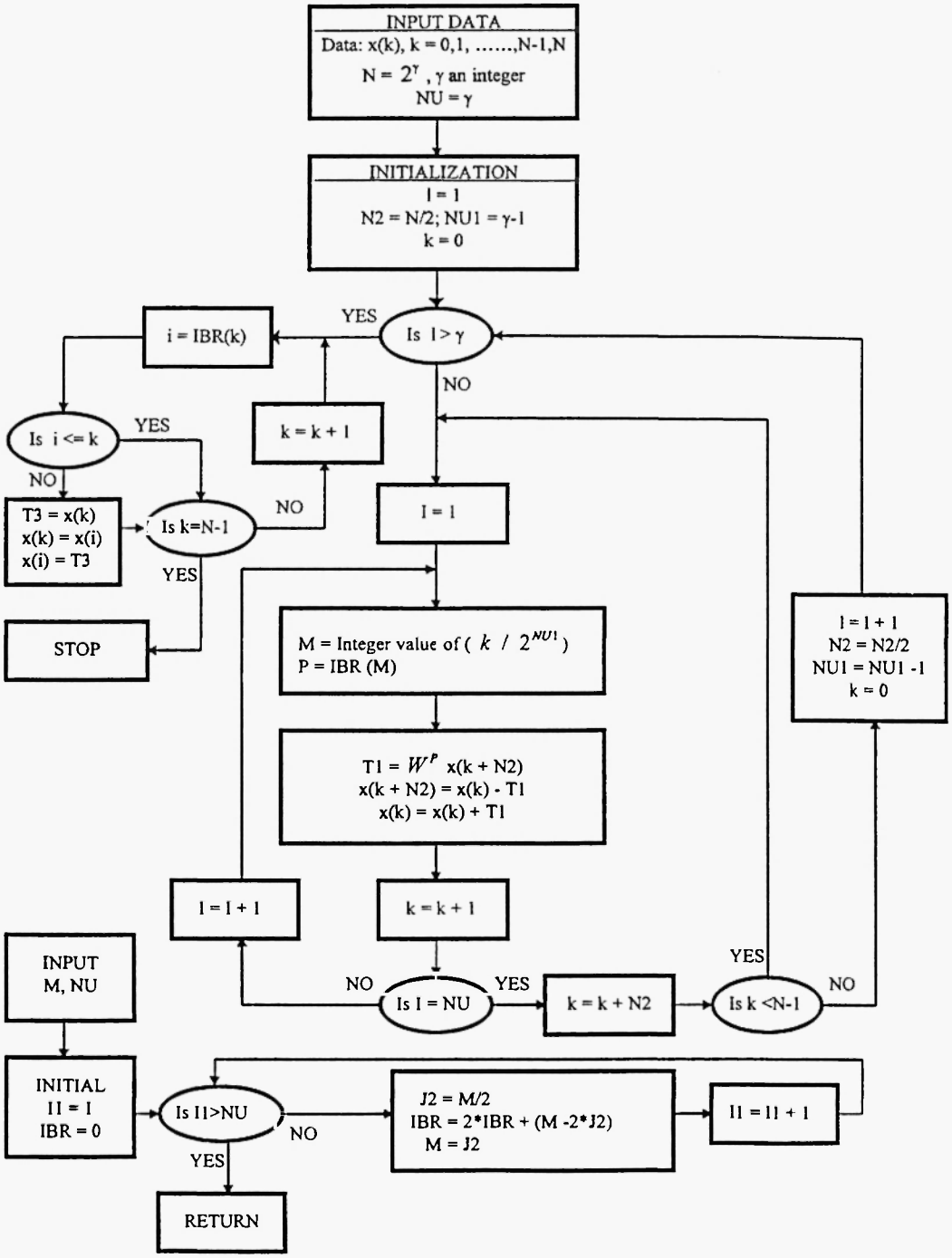
INPUT DATA
Data: x(k), k = 0,1, ...,N-1,N
N = 2^γ , γ an integer
NU = γ
INITIALIZATION
I = 1
N2 = N/2; NU1 = γ-1
k = 0
Is I > γ
YES
NO
i = IBR(k)
Is i <= k
YES
NO
k = k + 1
T3 = x(k)
x(k) = x(i)
x(i) = T3
Is k=N-1
NO
YES
I = 1
STOP
M = Integer value of (k / 2^NU1)
P = IBR (M)
T1 = W^P x(k + N2)
x(k + N2) = x(k) - T1
x(k) = x(k) + T1
I = I + 1
N2 = N2/2
NU1 = NU1 -1
k = 0
I = I + 1
k = k + 1
INPUT
M, NU
NO
Is I = NU
YES
k = k + N2
YES
Is k <N-1
NO
INITIAL
II = 1
IBR = 0
Is II>NU
NO
YES
J2 = M/2
IBR = 2*IBR + (M -2*J2)
M = J2
II = II + 1
RETURN